Mechanics Research Communications 134 (2023) 104200

Contents lists available at ScienceDirect

Mechanics Research Communications

journal homepage: www.elsevier.com/locate/mechrescom

Bandgap widening and resonator mass reduction through wave locking

L. Iorio *, J.M. De Ponti, A. Corigliano, R. Ardito

Department of Civil and Environmental Engineering, Politecnico di Milano, Piazza Leonardo da Vinci, 32, 20133 Milano, Italy

ARTICLE INFO

Keywords:
Vibration isolation
Bandgap
Local resonance
Wave locking
Wave coupling

ABSTRACT

Elastic metamaterials made of locally resonant arrays have been developed as effective ways to create band gaps for elastic or acoustic travelling waves. They work by implementing stationary states in the structure that localise and partially reflect waves. A different, simpler, way of obtaining band gaps is using phononic crystals, where the generated band gaps come from the periodic reflection and phase cancellation of travelling waves. In this work a different metamaterial structure that generates band gaps by means of coupling two contra-propagating modes is reported. This metamaterial, as it will be shown numerically and experimentally, generates larger band gaps with lower added mass, providing benefits for lighter structures.

1. Introduction

In the last decades, the study and development of metamaterials both in the photonic [1,2] and phononic [3–5] community has become an interesting topic for researchers. The curiosity for these novel structures comes from their intrinsic wave manipulation abilities even when the wavelength interacting with the structure is much larger than the lattice size. This enables novel properties for vibration attenuation [6–9], focusing and rerouting [10,11], non-reciprocity [12], or wave amplification for energy harvesting [13–15]. On the topic of vibration attenuation, numerous works have shown the potential and the advantages of using local resonators [16–21]. These structures generally consist of a main waveguide, that can be 1D (a beam) 2D (a plate) or 3D (a bulk solid), inside of which are placed local resonators. These resonators are capable of interacting with travelling waves by means of confining the traversing energy and creating a band gap at the frequency associated with their own resonance. It has been shown also, with analytical evaluations, that the extent of the band gap generated by these local structures mainly depends on the mass ratio between the locally resonant system (generally peripheral attachments) and the mass of the main waveguide structure. Moreover, the attenuation efficiency is heavily dependent on the number of cells employed as well as the relative stiffness between the resonators and the main structure [14,19,22]; the latter feature can also enable selective filtering of waves in metaframes [23]. The development of new metamaterial beams that implement exotic wave manipulation capabilities is very important for the creation of novel smart structures. New manipulation effects can modify the strength, the width and even the nature of band gaps that are introduced, granting tools for developing ever more efficient systems that can repel, localise or even damp out unwanted external or internal vibrations.

In this work, a metamaterial beam that can generate a band gap employing the so called locking effect [24–28] is proposed and evaluated. This different physical phenomenon, if properly implemented, can give new advantages for specific structures. For example, as it will be shown, the band gap can be greatly enlarged with respect to the simple local resonance counterpart, while reducing the added lateral mass. In the proposed design the band gap analysed is generated by the coupling of two contra-propagating modes (flexural and torsional) that interact thanks to a shift in position of the lateral resonators. This structure can significantly cut costs with regards to adding mass to the structure, giving also the benefit of having lighter metamaterial beams. This phenomenon can also be looked at from a different perspective: by considering an effective modification of inertial properties given by the rotation of the waveguide, that is slightly different with respect to what is commonly referred to as inertia amplification [29–34]. As a matter of fact, while for the local resonance structure the inertia is driven by translational motion due to flexure, this is enhanced in the case of locking by the rotational contribution introduced by torsion. The main difference with respect to classical inertial amplification systems is that the inertia amplification here considered is not just a geometrical effect, but a real augmentation of participating mass that comes from the motion of the main waveguide that participates in the resonators displacement. In the locking case we actually increase the mass by means of making not only the lateral resonators move but also part of the waveguide itself, which rotates with the resonators, increasing again the inertia.

* Corresponding author.
E-mail address: luca.iorio@polimi.it (L. Iorio).

https://doi.org/10.1016/j.mechrescom.2023.104200
Received 1 June 2023; Received in revised form 12 September 2023; Accepted 10 October 2023
Available online 12 October 2023

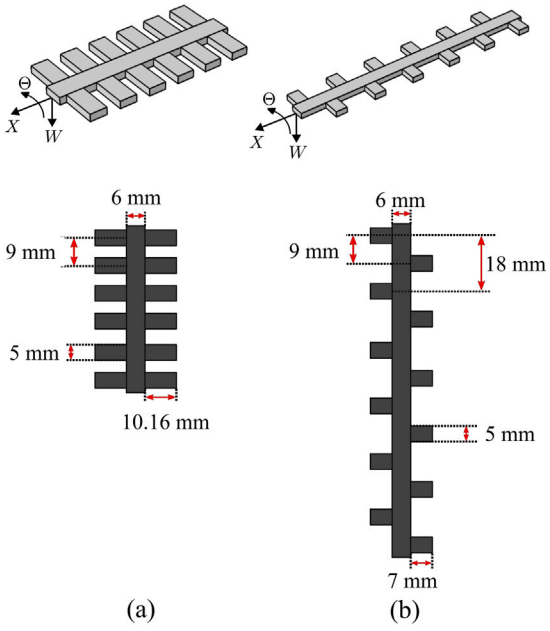

Fig. 1. Geometries analysed in this work: local resonance geometry (a) and locking geometry (b), with their respective vertical elevation. The thickness of both systems is $h = 2$ mm.

2. Analytical model

As stated above, the band gap developed for this metamaterial stems from the implementation of the locking effect in the main waveguide beam. Locking effect is the physical phenomenon that arises from the coupling of two contra-propagating waves with different polarisation. The coupling is responsible for the generation of at least one point of zero group velocity inside the first Brillouin zone and a band gap. The band gap is obtained through the looped energy conversion between one wave mode into another with opposite propagating direction. What is meant by "contra-propagating waves" is the existence of two distinct branches that have respectively a positive and a negative group velocity. This can be achieved by means of creating periodic arrays that, for the properties of periodic lattices, generate a certain wave periodicity that mirrors the branches thanks to the properties of the Brillouin zone. By just tuning the dimension of the periodic cell and the geometric and material properties one can engineer where two distinct branches have a point in common in the frequency-wavevector space. Under normal circumstances (when there is a preservation of symmetry in the structure) the two branches maintain a single point of accidental degeneracy, but when the symmetry is revoked the degeneracy gets lifted and a locking band gap is generated. This lifted degeneracy generates always two points of zero group velocity that can be either inside or, in rare cases, at the boundary of the IBZ. The lift in degeneracy and the band gap can be achieved only when the geometry of the structure allows one wave mode to interact with a different mode, in our case we achieve this by breaking symmetry and allowing flexural and torsional wave to interact thanks to the unbalanced motion of the resonators. The looped energy conversion, this refers to the fact that the two modes start to pass energy to one another during propagation in the beam, but, given the opposite propagation direction, the energy is somewhat trapped in the structure. This determines a complete reflection of the propagating wave energy if the frequency is higher than the one associated to the zero group velocity point [26,28]. The conventional local resonance, which is at the base of the commonly engineered passive metamaterials, on the other hand, arises from the coupling between a propagating mode and a stationary mode. In this paper, we compare two similar devices that show the aforementioned physical phenomena. In both cases, the waveguide is represented by an Euler–Bernoulli beam, on which resonators are attached in the form of cantilever beams. To achieve classical local resonance, the resonators are located in a symmetric fashion with respect to the beam's axis, see Fig. 1(a); conversely, wave locking can be achieved by introducing alternate resonators on a single side of each cell, see Fig. 1(b). In the analytical model we assume, for the sake of simplicity, that the motion of the resonator is dominated by the first eigenmode of the cantilever; this allows to adopt a spring–mass idealisation [28,35]. Consequently, the dynamic equilibrium of each resonator is established in terms of the equivalent bending stiffness k and the participating mass m. The reaction force F_n and the reaction moment M_n at the attachment point of each resonator are given by:

$$\begin{aligned} F_n &= k\left[\psi_n - \left(w_n + (-1)^n \theta_n \frac{b+\hat{L}}{2}\right)\right] \\ M_n &= F_n \frac{\hat{L}}{2}, \end{aligned} \tag{1}$$

where: $\psi_n = \psi_n(t)$ is the degree of freedom that describes the motion of the nth resonator; $w_n = w(nd,t)$ is the transverse displacement of the waveguide in correspondence of the nth resonator; $\theta_n = \theta(nd,t)$ is the torsional rotation of the waveguide in correspondence of the nth resonator; b is the width of the beam while $\hat{L}$ is the length of the resonator. The equation of motion for each resonator is written as:

$$\frac{\partial^2 \psi_n}{\partial t^2} + \omega_0^2 \left[\psi_n - \left(w_n + (-1)^n \theta_n \frac{b+\hat{L}}{2}\right)\right] = 0. \tag{2}$$

The eigenfrequency of the resonator is denoted by $\omega_0 = \sqrt{k/m}$.

The equation of motion of the waveguide is written in different form for the two devices. For the case of classic local resonance, in view of the symmetric distribution of resonators, the torsional rotation is null, whereas the equilibrium in the transverse direction contains the contribution of the two resonators in each cell:

$$\begin{aligned} EI\frac{\partial^4 w}{\partial x^4} + \rho A \frac{\partial^2 w}{\partial t^2} &= \sum_{n=-\infty}^{n=+\infty} 2F_n \delta(x - nd) \\ \theta &= 0. \end{aligned} \tag{3}$$

In the above equation, E is the Young's modulus and ρ is the mass density of the material of the waveguide; A and I represent the area and the moment of inertia of its cross-section, respectively; δ is the Dirac's delta.

In the case of wave locking, the asymmetric configuration entails the coupling with torsional behaviour, so that the equations of motion read:

$$\begin{aligned} EI\frac{\partial^4 w}{\partial x^4} + \rho A \frac{\partial^2 w}{\partial t^2} &= \sum_{n=-\infty}^{n=+\infty} F_n \delta(x - nd) \\ GJ\frac{\partial^2 \theta}{\partial x^2} - \rho I_p \frac{\partial^2 \theta}{\partial t^2} &= -\sum_{n=-\infty}^{n=+\infty} (-1)^n F_n \frac{b+\hat{L}}{2} \delta(x - nd). \end{aligned} \tag{4}$$

where: G is the tangential modulus of the material; I_p and J are the polar moment of inertia and the (primary) torsional stiffness of the cross-section, respectively.

The systems of Eqs. (1), (2), (3) and (1), (2), (4) can be solved by adopting the plane-wave expansion method (PWEM), as explained in [28]. The analytical solution is useful in order to design the devices with the same opening frequency of band gap. As shown in Fig. 1, we assume the same cross-section, 6×2 mm^2, for the waveguide and the same dimension, $d = 9$ mm, of the unit cell. The cross-section of the lateral resonators is also the same, but their length is different. We assume a predefined value, $L_b = 7$ mm, for the system that shows wave locking and, by examining the analytical dispersion curve, we obtain the value $L_a = 10.16$ mm, in order to match the band gap opening frequency. As a result, we obtain that for wave locking the resonators are 31.10% shorter than the classical resonance case.

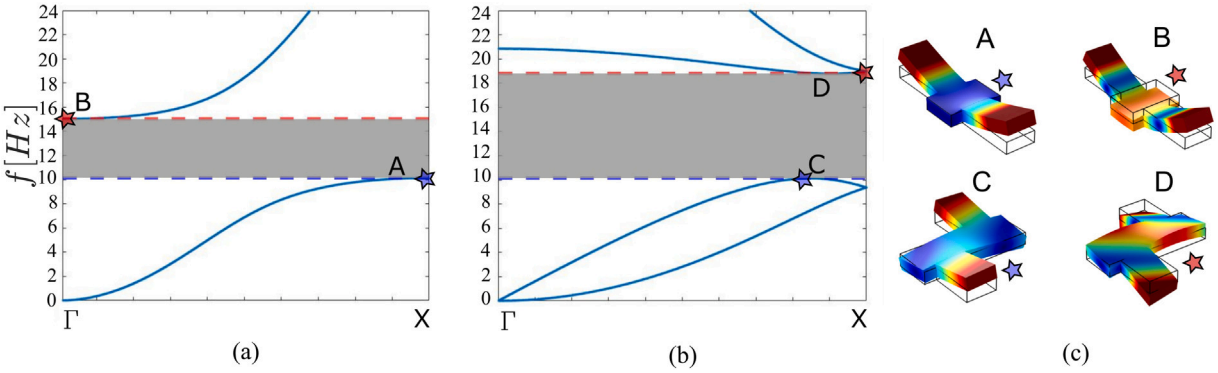

Fig. 2. (a) Dispersion relation for the local resonance geometry. (b) Dispersion relation for the locking geometry. The opening and closing of the band gaps are reported as dashed coloured lines, while in light grey the band gap zone is highlighted. (c) Reports of the eigensolutions associated to the highlighted frequencies. (For interpretation of the references to colour in this figure legend, the reader is referred to the web version of this article.)

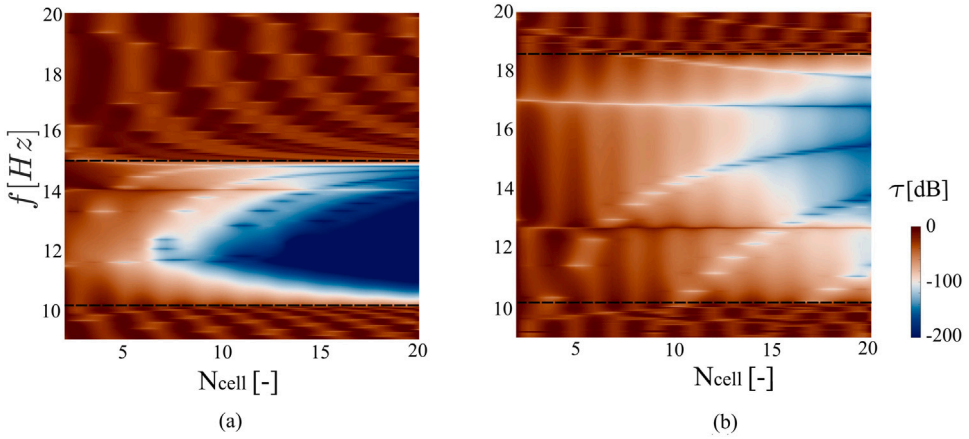

Fig. 3. Evaluation of the attenuation granted by the two metamaterials in the band gap region, varying the number of cells considered. (a) and (b) report the locally resonant case and the locking case, respectively. Dashed black horizontal lines report the theoretical opening and closing of the band gaps.

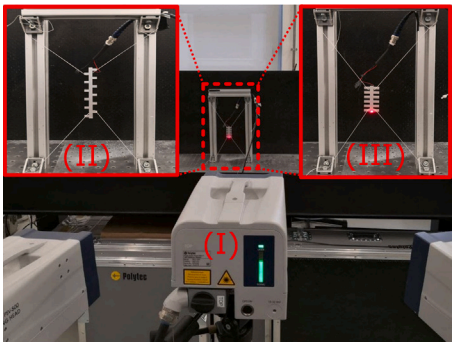

Fig. 4. Picture of the experimental setup: (I) marks one of the three heads of the vibrometer, (II) is the locking specimen, while (III) is the local resonance specimen.

3. Numerical analyses and results

The numerical analyses now reported are all conducted using the commercial software COMSOL Multiphysics, with the 3-dimensional modelling of the devices shown in Fig. 1. The material used for both configurations is aluminum (E = 70 GPa, ρ = 2710 kg/m^3, ν = 0.33). The elements used are second order hexahedrons with at least 4 elements on the shortest dimension (in our case the thickness of the main beam and resonators). The analyses performed numerically are: (1) eigenfrequency with Bloch–Floquet boundary conditions to obtain the dispersion relations and (2) frequency domain analyses to get the steady state response of the structures.

Fig. 2 reports the dispersion relation for the two geometries. In the locking case there is a clear coupling between the first flexural mode and the first torsional mode and this in turns generates the band gap. The coupling is granted by the shift in position of the resonators breaking the symmetry of the cell. The locking effect is more complicated to engineer with respect to conventional local resonance or Bragg scattering in a phononic crystal, because of the need to tailor the cell geometry (the resonator, the length of the cell and so on) so that in the reciprocal space there is a liftable accidental degeneracy of two contra propagating modes. This is particularly difficult to obtain at low frequencies. The dispersion shows that the opening frequency for the band gap of the two geometries is the same (10 156 Hz) while the closing frequency is very different: for the local resonance geometry the closing frequency is 15 012 Hz, while for the locking geometry it closes at 18 788 Hz. The gap-mid gap ratio is then evaluated to obtain a non-dimensional parameter that avoids frequency dependence. The formula is:

$$BG = \frac{2(f_{top} - f_{bot})}{f_{top} + f_{bot}} \cdot 100\% \tag{5}$$

where f_{bot} and f_{top} are the frequencies that delimit the band gap. From Eq. (5) it is obtained that the local resonance case has a gap-mid gap ratio of 38.56%, while for the locking it is 59.65%. Given that the overall added mass per cell is reduced by 31.10% this is an improvement in the effectiveness at creating bigger band gaps, reducing the added mass to the structure. These results may be explained by

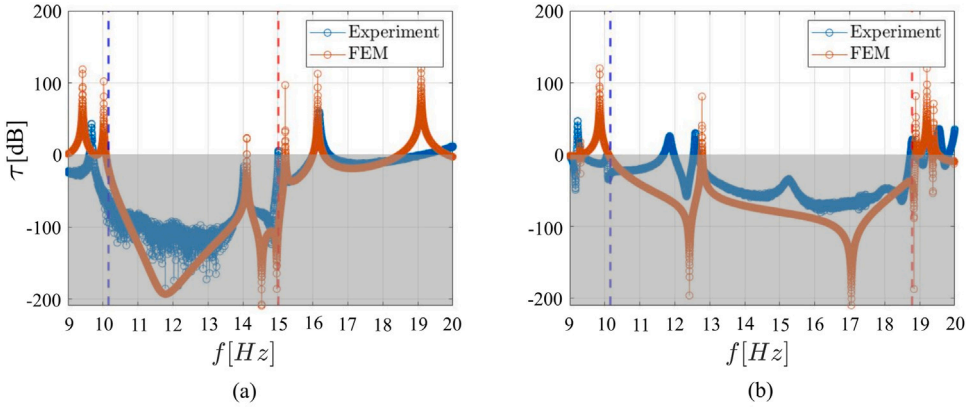

Fig. 5. Evaluation of the transmission in dB for the two structures subjected to the same sweep in frequency. We reported both the experimental outcomes solutions and the numerical results obtained with the finite element methods. (a) and (b) are respectively the results for local resonance and locking systems.

considering that the actual resonant masses in the two systems are different. The local resonance has just the lateral resonators as participants of the resonant motion, effectively being the only resonant masses of the modes. The locking case, on the other hand, employs not only the mass of the lateral resonators, but also the entire structure in the motion of the evaluated modes.

Fig. 3 now reports the analyses conducted to evaluate the effectiveness of the band gap. The attenuation capability given by the metamaterial at different frequencies is evaluated by means of a frequency sweep in the frequency domain analysis. Combining it with a second sweep of the number of cells provides us a clear indication on both where the band gap is and how many cells are needed to obtain an effective attenuation. We conclude that the attenuation capability of the locally resonant material is significantly higher with respect to the locking case for the same number of cells. This means that even though the band gap may be bigger, the attenuation is less efficient. As stated in previous research [19], for a small number of cells the band gap is larger with respect to the one defined by the dispersion relation (even though the attenuation is almost negligible), then, increasing the number of cells, the band gap shrinks and its opening and closing frequencies become defined. This is also true for the locking configuration, but it seems that the number of cells required for the stability of the band gap is lower, given that the boundaries are well defined already at eight cells.

To test the results obtained though finite element simulations, experiments with real specimens are also performed. The specimens are fabricated by means of laser cutting an aluminum plate of the desired thickness. The number of elementary cells that are sufficient for the desired properties is six. This was done analysing the preliminary numerical results. The experimental setup is as follows: the specimens are hanged from vertical supports to have free ended boundary conditions. A piezoelectric patch PZT-5H ($E_p = 61$ GPa, $\nu_p = 0.31$, $\rho_p = 7800$ kg/m^3 with dielectric constant $\epsilon_{33}^T/\epsilon_0 = 3500$ and piezoelectric coefficient $e_{31} = -9.2$ C/m^2) is attached to one end and it is used to supply the flexural excitation. The attenuation is then evaluated by extracting the out-of-plane velocity of the points at the centre line of the metamaterial beam thanks to a Polytec 3D Scanner Laser Doppler Vibrometer (SLDV). Fig. 4 shows the setup of the laboratory and the specimens. The results are reported in Fig. 5 for both metamaterial beams correlated with their respective finite element simulations. It is clear that the band gaps predicted by the numerical simulations are also present in the specimens produced. The band gaps reported both numerically and experimentally are not covering fully the regions predicted, meaning that there are some frequencies that are less or not at all attenuated. This is due to the boundary conditions and to the nature of the finite system that generate structural modes that are in the band gap. Furthermore we assess again that the local resonance band gap is more efficient in damping even in the experiment with respect to the locking band gap. Overall, it seems that the numerical results describe accurately the systems, the locking case seems to have some more not predicated global resonances but it could be expected given the more complicated phenomenon that can be perturbed by the not perfect boundary conditions.

4. Conclusions

In conclusion, a design concept for a vibration isolation meta-beam has been reported. With it, the analyses have shown that the subtraction of mass and the breaking of the symmetry in the position of the resonators grants the creation of larger, but slightly less efficient band gaps. This works even for structures that employ a limited number of cells. The downside of this lower attenuation capability is given by the significantly lower added mass. Furthermore the cell geometry is more limiting with respect to the local resonance case given the need of bigger cells and the more complicated engineering of the modes that have to be bent in the right way in order to obtain the locking effect and consequentially the band gap. Further studies of these locking designs could lead to new generations of metalattices and metaframes for further advancements of vibration isolation frames.

Declaration of competing interest

The authors declare that they have no known competing financial interests or personal relationships that could have appeared to influence the work reported in this paper.

Data availability

Data will be made available on request.

Acknowledgements

The support of the H2020 FET-proactive project MetaVEH under grant agreement No. 952039 is acknowledged.

References

[1] J.B. Pendry, Negative refraction makes a perfect lens, Phys. Rev. Lett. 85 (18) (2000) 3966.
[2] J.B. Pendry, A.J. Holden, D.J. Robbins, W. Stewart, Magnetism from conductors and enhanced nonlinear phenomena, IEEE Trans. Microw. Theory Tech. 47 (11) (1999) 2075–2084.
[3] R.V. Craster, S. Guenneau, Acoustic Metamaterials: Negative Refraction, Imaging, Lensing and Cloaking, Vol. 166, Springer Science & Business Media, 2012.
[4] Z. Liu, X. Zhang, Y. Mao, Y. Zhu, Z. Yang, C.T. Chan, P. Sheng, Locally resonant sonic materials, Science 289 (5485) (2000) 1734–1736.

[5] A.O. Krushynska, D. Torrent, A.M. Aragón, R. Ardito, O.R. Bilal, B. Bonello, F. Bosia, Y. Chen, J. Christensen, A. Colombi, S.A. Cummer, B. Djafari-Rouhani, F. Fraternali, P.I. Galich, P.D. Garcia, J. Groby, S. Guenneau, M.R. Haberman, M.I. Hussein, S. Janbaz, N. Jiménez, A. Khelif, V. Laude, M.J. Mirzaali, P. Packo, A. Palermo, Y. Pennec, R. Picó, M.R. López, S. Rudykh, M. Serra-Garcia, C.M. Sotomayor Torres, T.A. Starkey, V. Tournat, O.B. Wright, Emerging topics in nanophononics and elastic, acoustic, and mechanical metamaterials: An overview, Nanophotonics 12 (4) (2023) 659–686.

[6] L. D'Alessandro, A.O. Krushynska, R. Ardito, N.M. Pugno, A. Corigliano, A design strategy to match the band gap of periodic and aperiodic metamaterials, Sci. Rep. 10 (1) (2020) 16403.

[7] J.M. De Ponti, N. Paderno, R. Ardito, F. Braghin, A. Corigliano, Experimental and numerical evidence of comparable levels of attenuation in periodic and a-periodic metastructures, Appl. Phys. Lett. 115 (2019).

[8] D. Colquitt, A. Colombi, R. Craster, P. Roux, S. Guenneau, Seismic metasurfaces: Sub-wavelength resonators and rayleigh wave interaction, J. Mech. Phys. Solids 99 (2017) 379–393.

[9] A.O. Krushynska, M. Miniaci, F. Bosia, N.M. Pugno, Coupling local resonance with bragg band gaps in single-phase mechanical metamaterials, Extreme Mech. Lett. 12 (2017) 30–36.

[10] S. Tol, F.L. Degertekin, A. Erturk, Phononic crystal luneburg lens for omnidirectional elastic wave focusing and energy harvesting, Appl. Phys. Lett. 111 (2017).

[11] A. Colombi, R. Craster, D. Colquitt, Y. Achaoui, S. Guenneau, P. Roux, M. Rupin, Elastic wave control beyond band-gaps: Shaping the flow of waves in plates and half-spaces with subwavelength resonant rods, Front. Mech. Eng. 3 (2017).

[12] A. Rakhimzhanova, M. Brun, Direction-selective non-reciprocal mechanical energy splitter, Phil. Trans. R. Soc. A 380 (2022).

[13] M. Alshaqaq, A. Erturk, Graded multifunctional piezoelectric metastructures for wideband vibration attenuation and energy harvesting, Smart Mater. Struct. 30 (1) (2020) 015029.

[14] J.M. De Ponti, Graded Elastic Metamaterials for Energy Harvesting, Springer, 2021.

[15] J.M. De Ponti, L. Iorio, E. Riva, F. Braghin, A. Corigliano, R. Ardito, Enhanced energy harvesting of flexural waves in elastic beams by bending mode of graded resonators, Front. Mater. 8 (2021).

[16] H. Sun, X. Du, P.F. Pai, Theory of metamaterial beams for broadband vibration absorption, J. Intell. Mater. Syst. and Struct. 21 (11) (2010) 1085–1101.

[17] D. Yu, Y. Liu, H. Zhao, G. Wang, J. Qiu, Flexural vibration band gaps in euler-bernoulli beams with locally resonant structures with two degrees of freedom, Phys. Rev. B 73 (6) (2006) 064301.

[18] Y. Xiao, J. Wen, D. Yu, X. Wen, Flexural wave propagation in beams with periodically attached vibration absorbers: Band-gap behavior and band formation mechanisms, J. Sound Vib. 332 (4) (2013) 867–893.

[19] C. Sugino, S. Leadenham, M. Ruzzene, A. Erturk, On the mechanism of bandgap formation in locally resonant finite elastic metamaterials, J. Appl. Phys. 120 (13) (2016) 134501.

[20] A. Dwivedi, A. Banerjee, S. Adhikari, B. Bishakh, Bandgap merging with double-negative metabeam, Mech. Res. Commun. 122 (2022).

[21] L.S. Prado, T.G. Ritto, Vibration reduction of a rotating machine using resonator rings, Mech. Res. Commun. 107 (2020).

[22] M.I. Hussein, M.J. Leamy, M. Ruzzene, Dynamics of phononic materials and structures: Historical origins, recent progress, and future outlook, Appl. Mech. Rev. 66 (4) (2014).

[23] J.M. De Ponti, E. Riva, F. Braghin, R. Ardito, Elastic three-dimensional metaframe for selective wave filtering and polarization control, Appl. Phys. Lett. 119 (21) (2021) 211903.

[24] J.L. du Bois, N.A. Lieven, S. Adhikari, Localisation and curve veering: a different perspective on modal interactions, in: Proceedings of the 27th International Modal Analysis Conference, 2009.

[25] P.-T. Chen, J. Ginsberg, On the relationship between veering of eigenvalue loci and parameter sensitivity of eigenfunctions, J. Vib. Acoust. 114 (2) (1992) 141–148.

[26] B.R. Mace, E. Manconi, Wave motion and dispersion phenomena: Veering, locking and strong coupling effects, J. Acoust. Soc. Am. 131 (2) (2012) 1015–1028.

[27] G. Trainiti, J. Rimoli, M. Ruzzene, Wave propagation in periodically undulated beams and plates, Int. J. Solids Struct. 75-76 (2015) 260–276.

[28] J.M. De Ponti, L. Iorio, E. Riva, R. Ardito, F. Braghin, A. Corigliano, Selective mode conversion and rainbow trapping via graded elastic waveguides, Phys. Rev. A 16 (2021) 034028.

[29] R. Zaccherini, A. Colombi, A. Palermo, H.R. Thomsen, E.N. Chatzi, Stress-optimized inertial amplified metastructure with opposite chirality for vibration attenuation, 2021, arXiv preprint arXiv:2111.08594.

[30] C. Yilmaz, G.M. Hulbert, N. Kikuchi, Phononic band gaps induced by inertial amplification in periodic media, Phys. Rev. B 76 (5) (2007) 054309.

[31] G. Acar, C. Yilmaz, Experimental and numerical evidence for the existence of wide and deep phononic gaps induced by inertial amplification in two-dimensional solid structures, J. Sound Vib. 332 (24) (2013) 6389–6404.

[32] M. Mazzotti, A. Foehr, O.R. Bilal, A. Bergamini, F. Bosia, C. Daraio, N.M. Pugno, M. Miniaci, Bio-inspired non self-similar hierarchical elastic metamaterials, Int. J. Mech. Sci. 241 (2023) 107915.

[33] M. Miniaci, M. Mazzotti, A. Amendola, F. Fraternali, Effect of prestress on phononic band gaps induced by inertial amplification, Int. J. Solids Struct. 216 (2021) 156–166.

[34] A. Bergamini, M. Miniaci, T. Delpero, D. Tallarico, B. Van Damme, G. Hannema, I. Leibacher, A. Zemp, Tacticity in chiral phononic crystals, Nat. Commun. 10 (1) (2019) 4525.

[35] E.A. Skelton, R.V. Craster, A. Colombi, D.J. Colquitt, The multi-physics metawedge: graded arrays on fluid-loaded elastic plates and the mechanical analogues of rainbow trapping and mode conversion, New J. Phys. 20 (5) (2018) 053017.